COMBUSTION ENGINES

Reduction of Friction & Wear

COMBUSTION ENGINES— REDUCTION OF FRICTION AND WEAR

IMechE CONFERENCE PUBLICATIONS 1985–3

Sponsored by
The Power Industries Division of
The Institution of Mechanical Engineers and
The Japanese Society of Mechanical Engineers

18–19 March 1985
1 Birdcage Walk, Westminster, London SW1

Published for
The Institution of Mechanical Engineers
by Mechanical Engineering Publications Limited
LONDON

First published 1985

British Library Cataloguing in Publication Data

Combustion engines: reduction of friction and wear: papers read at the conference held at the Institution of Mechanical Engineers, London on 18–19 March 1985.
1. Combustion engineering
I. Institution of Mechanical Engineers, *Power Industries Division* II. Nihon kikaigakkai
621.402'3 TJ254.5

ISBN 0 85298 559 2

Printed by Waveney Print Services Ltd, Beccles, Suffolk

Conference Planning Panel

M L Monaghan, CEng, FIMechE (Chairman)
Ricardo Consulting Engineers plc
Shoreham-by-Sea
West Sussex

R Douglas, PhD, AMIMechE
Ford Motor Company Limited
Basildon
Essex

R F Haycock, ARCS
Esso Chemicals Research Centre
Abingdon
Oxfordshire

C M D Little, CEng, MIMechE
Lucas Bryce Limited
Hucclecote
Gloucester

C M Taylor, PhD, CEng, MIMechE
Institute of Tribology
Department of Mechanical Engineering
University of Leeds

R Thomas
Rolls-Royce Motors Limited
Shrewsbury
Shropshire

K L Walker, MA
Perkins Engines Company
Peterborough
Cambridgeshire

K W Wright
Rolls-Royce Aero Division
Derby
Derbyshire

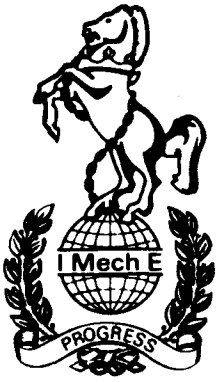

The Institution of Mechanical Engineers

The primary purpose of the 76,000-member Institution of Mechanical Engineers, formed in 1847, has always been and remains the promotion of standards of excellence in British mechanical engineering and a high level of professional development, competence and conduct among aspiring and practising members. Membership of IMechE is highly regarded by employers, both within the UK and overseas, who recognise that its carefully monitored academic training and responsibility standards are second to none. Indeed they offer incontrovertible evidence of a sound formation and continuing development in career progression.

In pursuit of its aim of attracting suitably qualified youngsters into the profession — in adequate numbers to meet the country's future needs — and of assisting established Chartered Mechanical Engineers to update their knowledge of technological developments — in areas such as CADCAM, robotics and FMS, for example — the IMechE offers a comprehensive range of services and activities. Among these, to name but a few, are symposia, courses, conferences, lectures, competitions, surveys, publications, awards and prizes. A Library containing 150,000 books and periodicals and an Information Service which uses a computer terminal linked to databases in Europe and the USA are among the facilities provided by the Institution.

If you wish to know more about the membership requirements or about the Institution's activities listed above — or have a friend or relative who might be interested — telephone or write to IMechE in the first instance and ask for a copy of our colour 'at a glance' leaflet. This provides fuller details and the contact points — both at the London HQ and IMechE's Bury St Edmunds office — for various aspects of the organisation's operation. Specifically it contains a tear-off slip through which more information on any of the membership grades (Student, Graduate, Associate Member, Member and Fellow) may be obtained.

Corporate members of the Institution are able to use the coveted letters 'CEng, MIMechE' or 'CEng, FIMechE' after their name, designations instantly recognised by, and highly acceptable to, employers in the field of engineering. There is no way other than by membership through which they can be obtained!

CONTENTS

C67/85

Friction in internal combustion engine bearings

F A MARTIN, CEng, FIMechE
The Glacier Metal Company Limited, Ealing Road, Alperton, Wembley, Middlesex

SYNOPSIS

Bearing friction forms a significant part of the total mechanical losses within an engine. Reduction in these losses will help with energy conservation. Various techniques, used internationally, for predicting bearing friction are reviewed. The effect of bearing size, bearing shape, oil feed grooving, viscosity and environmental effects are discussed. Many of these factors are incorporated in power loss prediction charts and trend analysers. Examples of friction reduction in redesigned engines are given.

1. INTRODUCTION

The need for energy conservation has meant that a deeper understanding is required of the mechanisms of friction losses within all components of an internal combustion engine. In the automotive field it has been estimated that a 10% reduction in the direct mechanical losses within an engine gives perhaps 1 to 3% improvement in fuel consumption. Such savings are very significant when viewed on a worldwide basis, in both economic and conservation terms. For these reasons many manufacturers, particularly in Japan and USA (1, 2, 3, 4) have gained improvements in fuel economy by reducing the mechanical friction losses within the engine by careful re-design. Bearings are one component which contributes to the overall friction losses, and this paper reviews the current knowledge on bearing design as it relates to friction losses, and attempts to correlate the work of many researchers.

The calculation of friction losses within a bearing oil film is an integral part of the design process for that bearing. These losses, appearing as heat, raise the temperature of the lubricant within the clearance space, and lower its operating viscosity. This change in viscosity heavily influences the oil film thicknesses within the bearing throughout the entire journal orbit, which in turn feed back into modified power losses. Therefore an accurate assessment of bearing friction is a necessity in its own right when carrying out any detailed design work on engine bearings. Techniques for predicting such orbits were described by the author in a basic review (5) which has recently been updated (6). In order to be able to compare different prediction methods a particularly well documented bearing has been taken as a study case in these and other papers. This same bearing (the big end of a Ruston and Hornsby VEB MK III 600hp 600 rev/min diesel engine) has been used in this present review paper to compare friction calculation methods. In particular, studies have been carried out by the Glacier Metal Company and GEC in England, and General Motor Research Laboratories in the USA. Also fundamental data from Delft and Twente Universities in the Netherlands and Cornell University in the USA have been used.

In order to give some help with the initial design of bearing systems, an attempt has been made to give guidance on the effect of various bearing and environmental factors on friction losses. In this work the basic bearing dimensions of diameter, length and clearance have been related to the choice of lubricant viscosity within the bearing, and the relative values of the rotating and reciprocating masses within the engine. Prediction charts are presented which are based on many diverse theoretical studies, and comparisons are made with experiments on motored engines.

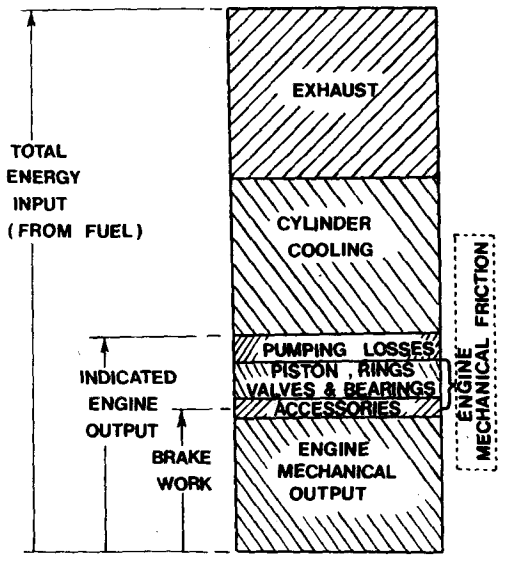

Fig 1 Typical energy distribution in an automotive engine (Petrol engine — part open throttle)

2 NOTATION

General

b	=	bearing length	(m)
c or c_r	=	radial clearance	(m)
C_d	=	diametral clearance	(m)
d	=	bearing diameter	(m)
e	=	eccentricity	(m)
F	=	bearing load	(N)
F_F	=	friction force	(N)
h	=	film thickness	(m)
H	=	Power loss	(W)
N	=	Rotational speed	(rev/s)
P	=	Specific load	(N/m^2)
R	=	Crank throw	(m)
η	=	Operating viscosity	(Ns/m^2)
θ	=	angle from h_{max}	(deg)

Relating to Power Loss Equation - (Tables 1, 2, Fig 6)

H_{ROT}	=	Power loss due to rotation	(W)
H_{TRANS}	=	Power loss due to translation	(W)
H_{TOTAL}	=	$H_{ROT} + H_{TRANS}$	(W)
F_j	=	Force applied to oil film by the journal	(N)
τ_j	=	Torque exerted on the oil film by the journal	(Nm)
τ_b	=	Torque exerted on the oil film by the bearing	(Nm)
ω_j	=	Angular velocity of journal	(rad/s)
ω_b	=	Angular velocity of bearing	(rad/s)
ϕ	=	Angle measured from F_j to h_{min} position	(deg)
β	=	Angle measured from F_j to $\underline{V}$	(deg)
V	=	Journal centre velocity (ref x,y frame)	(m/s)

Relating to Inertia Study (Figs 8 and 9)

A, B and C - load diagram shape factors

F_c	=	Rotating inertia force	(N)
P_c	=	Specific load $F_c/(bd)$	(N/m^2)
M_c	=	Rotating mass	(kg)
M_I	=	Reciprocating mass	(kg)

Dimensionless Terms (in consistent units)

Coefficient of friction $f = \frac{F_F}{F}$ or $\frac{F_F}{F_c}$

Dimensionless power loss $H' = \frac{H\,C_d}{\eta\, bd^3N^2}$

Load Number $W'_c = \frac{P_c}{\eta\, N}\left(\frac{C_d}{d}\right)^2$

$= \frac{2\pi^2 M_c NR}{br\,\eta}\left(\frac{c}{r}\right)^2$

Eccentricity Ratio $\epsilon = e/c_r$

3. BEARING FRICTION AS PART OF THE ENERGY DISTRIBUTION

The energy distribution and friction in various engines have been the subject of detailed study by many researchers (1) (2) (3) (4) (7) (8). Information has been presented on both petrol and diesel engines, on low and high load conditions, and on part open and full open throttle conditions. More general reviews on the subject are given by Rosenberg (9) and Parker and Adams (10).

The mechanical friction losses in an engine are developed in the piston (skirt) and rings, the valve system, the bearing system, and those accessories directly associated with the engine. A typical energy distribution (see also Pinkus and Wilcock (11) Lang (12)) is shown in Fig 1 for a passenger car engine under part throttle operating conditions. This figure shows schematically that about 30% of the energy available within the fuel goes out to the exhaust, 30% is involved in cylinder cooling, with only 40% providing the indicated output. However, only 25% of the total energy is ultimately available as brake work (to transmission and road wheels) with mechanical friction and pumping losses accounting for the remainder. Summarizing, the engine mechanical losses account for -

8 to 10% of total energy input (total energy basis)
or 20 to 25% of indicated output (indicated output basis).

These figures cannot be totally general, and they will vary with operating conditions, type of engine etc. However, they do serve to show the scale of the friction loss within the engine. More detailed effects are shown by the experimental work at the Ford Motor Co (4) which illustrates the effect of full and part throttle conditions on mechanical friction. This is reproduced in Fig 2, and shows a greater proportion of mechanical losses at part throttle conditions; it indicates how the various engine components contribute to the friction losses, although pistons and bearings are considered together.

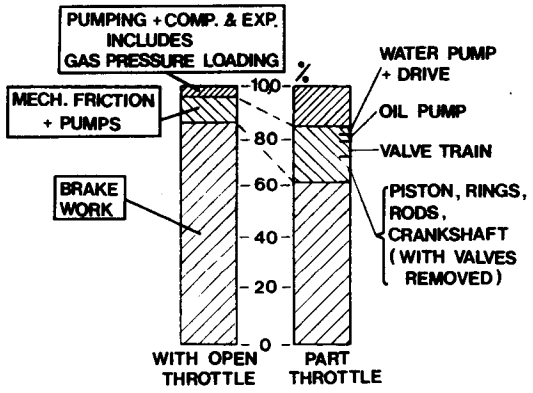

Fig 2 Effect of full and part throttle on engine friction
Ford Motor Company — Kovach et al (4)

Dr Lang of Daimler Benz, Germany, presented an overview of 'Friction losses in combustion engines' at the 1981 'Limits of Lubrication' Conference, and this talk has since been published (12). Lang states that the mechanical losses are approximately 25% of the energy in the cylinder, giving details in an excellent pictorial presentation, Fig 3. This is based on average values for engines with different numbers of cylinders, auxiliaries, types of combustion, speed and load. Some of these mechanical losses are attributed to auxiliaries such as water and oil pumps, cooling fan, generator, compressor and hydraulic pumps etc. According to Lang, friction losses which could be improved or optimised tribologically amount to about 72.5% of the mechanical losses, consisting of:-

valve train	6%
connecting rod bearings	10%
main bearings	12.5%
piston rings	19%
pistons	25%

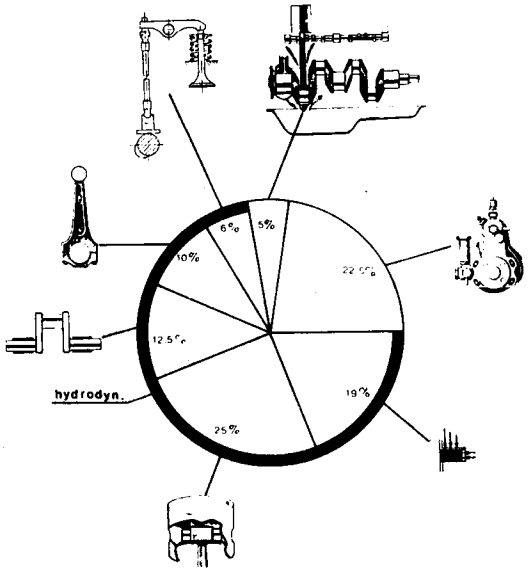

Fig 3 Mechanical losses in combustion engines, Lang (12)

Typical distributions of friction loss, associated with various engine components, recently formulated in the USA (4) and Japan (3) are shown in Fig 4 (a) and (b). These trends, showing friction mean effective pressure (proportional to friction torque) against engine speed, are from motored engines. It is difficult to see exactly the friction loss contribution of the bearings alone, since in the Ford experimental results, Fig 4 (a), seals are included with the crankshaft, and the piston assemblies are included with the connecting rod bearings. However, they do give a useful guide. The experiments from Fuji Heavy Industries Ltd, Fig 4(b), are more enlightening, since the losses within the piston system (generally forming a major part of the mechanical losses (12)), are considered separately.

Many other studies on motored friction (2) (7) (9) (10) (11) (13) are reported in the literature; in particular the work of Bishop (8) has formed a basic reference work over the past two decades. Taking a logical grouping of variables and using regression analysis techniques he gives a broad analytical guideline for a 'rough' but reasonable approximation of the various friction components, including the crankcase mechanical friction.

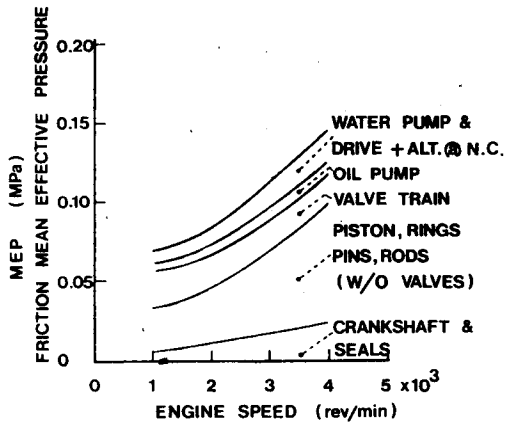

(a) Ford Motor Company — Kovach et al (4)

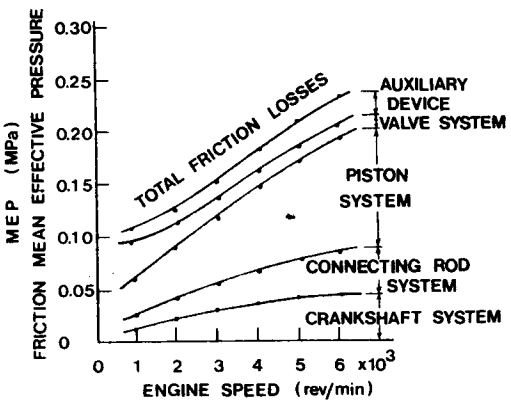

(b) Fuji Heavy Industries — Hoshi (3)

Fig 4 Examples of engine component friction from motored engines

4. PREDICTION OF BEARING FRICTION AND POWER LOSS

4.1 Some basic concepts considering a steady load

To obtain a physical appreciation of the mechanisms that control power loss in a bearing it is helpful to consider the steady load case shown in Fig 5. This particular analysis has been simplified by assuming that the load carrying film extends throughout the converging part of the clearance space (ie from h_{max} to h_{min} the so called π film extent). The figure shows how power loss (in dimensionless terms) varies with the journal eccentricity ratio.

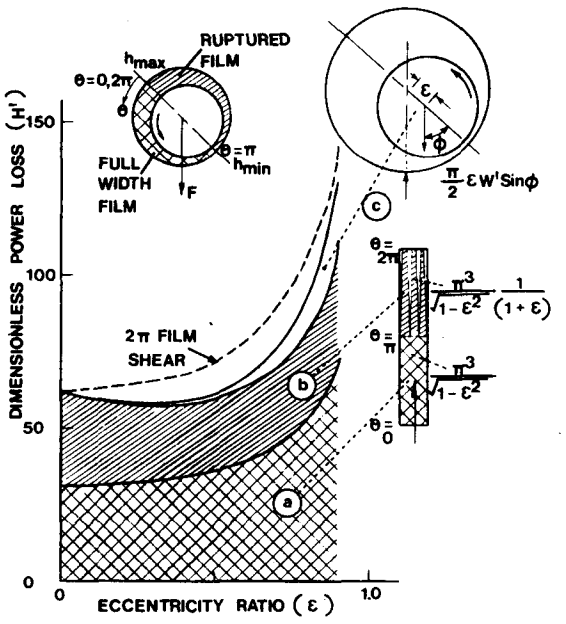

Fig 5 Schematic diagram showing power loss components for steady load conditions

Three effects labelled (a) (b) and (c) in Fig 5 control the power loss. The lower chequered area (labelled (a)) represents the shear losses generated in the full width film condition of the converging film; the dimensionless power loss for this region is a function of the eccentricity ratio:-

$$H' = \pi^2 c_r \int_{\theta=0}^{\theta=\pi} \frac{d\theta}{h} = \frac{\pi^3}{(1-\epsilon^2)^{0.5}} \qquad ..[1]$$

The second component (labelled (b)) is due to shear of the oil in the diverging region. Here a constant volume of oil (controlled by the cross section at h_{min}) is carried around circumferentially, splitting up into streamers; the power loss is dependent upon a modified function of eccentricity ratio.

The component marked (c) is due to the hydrodynamic film pressure (14) and is effectively a torque term; it is a function of journal position and load.

When the journal is concentric with the bearing ($\epsilon = 0$), the angular extent of the oil film will be 2π. The friction equation (14) for this case (sometimes called the Petroff equation) is given by:-

$$F_F = \frac{\text{shear area x viscosity x velocity}}{\text{film thickness}}$$

$$= \frac{2\pi r b \eta U}{c_r}$$

or in terms of power loss

$$H = F_F \omega r$$

$$= \frac{2\pi^3 \eta N^2 b d^3}{c_d}$$

or in terms of dimensionless power loss H' (see notation)

$$H' = 2\pi^3$$

(ie 62.0 on the vertical axis in Fig 5).

If shear effects only were taken, and it was assumed that a complete (non-ruptured) film occurred over the full eccentricity range then the losses shown by the "2π film shear" line would be predicted. It can be seen that oil film rupture lowers the bearing loss.

4.2 Dynamically loaded bearings

In dynamically loaded bearings the situation is much more complex. Whilst the load carrying film also extends just over 180^o for a finite bearing solution (apart from film history solution (15)) it is not, however, restricted to the converging wedge part of the film, because the dynamic case also relies on 'squeeze' action for the generation of film pressures. This is illustrated schematically by the various positions of the 180 degree load carrying film (approximate solution) shown in Fig A1 in the appendix. Consequently one cannot use the simple $(1-\epsilon^2)^{-0.5}$ term for friction in the load carrying film of engine bearings as the film is seldom from maximum to minimum film positions. As an expedient, a completely full 2π film is often considered in engine bearings (where there is symmetry of oil film extent about the line of journal and bearing centres). For this case the shear component is simply given as twice that in equation [1].

$$H' = 2\pi^3/(1 - \epsilon^2)^{0.50} \qquad ..[2]$$

The advantage of this equation is its simplicity. However, it does not allow for film rupture in the bearing, and this can be important. Other factors which should be considered when predicting power loss in engine bearings are:-

a) for big end (connecting rod) bearings the angular velocity of the big end bearing ω_b is not constant with time, and this should be considered together with the journal angular velocity ω_j

and b) the actual translatory motion of the journal centre within the bearing clearance space.

4.3 General friction torque and power loss equations for the dynamic load case

One of the most comprehensive equations for predicting power loss in bearings is given by Booker, Goenka and van Leeuwen (16) in vector and cross-product format. The author of this review paper agrees with the validity of this equation and has rearranged it into algebraic form to make it more understandable and so that it can be more readily compared with the work of others. A summary of such equations and their development are given in Tables 1 and 2, for the geometric notation* shown in Fig 6.

Table 1 – Rate of work done on oil film due to **Rotation** of journal and bearing

A + B	A Shear Term	B Pressure Term
Torque τ_j	$\eta r^3 \iint \frac{1}{h} d\theta dz \left[\omega_j - \omega_b\right]$	$r \iint \frac{h}{2} \frac{\partial P}{\partial \theta} d\theta dz$
τ_b	$-\eta r^3 \iint \frac{1}{h} d\theta dz \left[\omega_j - \omega_b\right]$	$r \iint \frac{h}{2} \frac{\partial P}{\partial \theta} d\theta dz$
Power Loss $\omega_j \tau_j$	$\eta \frac{r^3 b}{c} J_1^{oo} \left[\omega_j - \omega_b\right]\omega_j$	$\omega_j F_j \frac{e \sin \phi}{2}$
$\omega_b \tau_b$	$-\eta \frac{r^3 b}{c} J_1^{oo} \left[\omega_j - \omega_b\right]\omega_b$	$\omega_b F_j \frac{e \sin \phi}{2}$
$H_{ROT} = \omega_j \tau_j + \omega_b \tau_b$	$\eta \frac{r^3 b}{c} J_1^{oo} \left[\omega_j - \omega_b\right]^2$	$\left[\omega_j \frac{+\omega_b}{2}\right] F_j e \sin \phi$

Table 2 – Rate of work done on oil film due to **Translation** of journal centre O_j with respect to bearing centre O_b

C	Translatory Term C
Power Loss	
$H_{Trans} = \underline{F}_j \cdot \underline{V}$ where $\underline{V} = \left.\frac{d\underline{e}}{dt}\right\|_{x,y}$	$\underline{F}_j \cdot \underline{V} = \left\|\underline{F}_j\right\| \left\|\underline{V}\right\| \cos\beta$ $= F_j \; V \; \cos\beta$

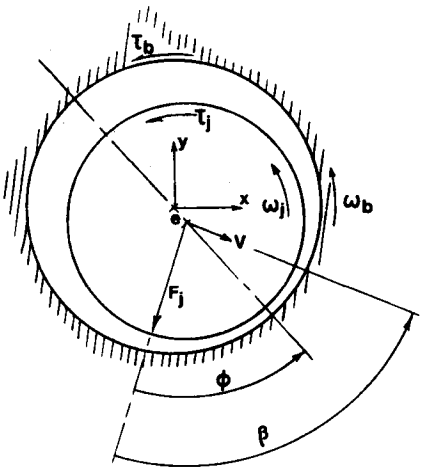

Fig 6 Notation for power loss equations in tables 1 & 2

Table 1 relates to the rate of work done on the oil film due to **rotation** of journal and bearing, resulting in a shear term A and a pressure term B. Table 2 relates to the work done on the oil film due to **translation** of the journal centre (term C).

The resulting power loss at any instant is given by:-

$$H = H_{Rot} + H_{Trans}$$

$$= \left[\frac{\eta r^3 b}{c} J_1^{oo} (\omega_j - \omega_b)^2 + (\omega_j \frac{+\omega_b}{2}) F_j \, e \sin\phi\right] + \left[F_j \, V \cos\beta\right] \quad \ldots.[3]$$

For a 180^o load carrying film (such as given by short bearing theory)

J_1^{oo} will be equal to $\int_{\theta_1}^{\theta_1+\pi} \frac{d\theta}{(1+\epsilon\cos\theta)}$

Values for this integration can be found in Booker's table of journal bearing integrals (17). The detailed form of the integration will depend on the attitude angle ϕ and whether the eccentricity is decreasing or increasing, as shown in the Appendix (Fig A1). For a completely full film (no film rupture) J_1^{oo} is simply

$$2\pi/(1 - \epsilon^2)^{0.5}$$

The power loss equation [3] gives a good basic foundation for further analysis and for comparing the work of others.

*Footnote – Both Booker and Martin define ϕ positive in a counter clockwise direction. However, Booker considers ϕ from $\underline{\epsilon}$ to $\underline{F}$ (as $\underline{\epsilon}$ is used as a reference axis) and Martin considers ϕ from $\underline{F}_j$ to $\underline{\epsilon}$ (to be consistent with the special case of a steadily loaded bearing). This results in $\phi_{Martin} = 2\pi - \phi_{Booker} = -\phi_{Booker}$ and is instrumental in transforming Booker's equation to those in Tables 1 and 2 as summarised in Table 3.

4.4 Different forms of prediction equations

Several terms make up the general power loss equation [3] and these can be made more applicable to particular situations by choosing the appropriate frame of reference. The friction losses due to shear will be the same irrespective of where an observer is placed, since the shear term involves the **difference** of two angular velocities. The total power loss is not affected by the choice of the reference frame and therefore the **sum** of the remaining terms, labelled 'pressure' and 'translation', will be unchanged, although they will vary individually depending on the motion of the observer (ie on the reference frame).

Such changes to the 'pressure' and 'translation' terms can be illustrated by an example case where the 'observer' is rotating at an average film velocity of $(\omega_j + \omega_b)/2$. For this case the 'pressure' term goes to zero and the 'translation' term will be the product of the force from the journal acting on the oil film F_j and the apparent velocity of the journal V_{ξ}^{j} parallel to the instantaneous load line. The resulting equation for this case is :-

$$\text{Power Loss} = \frac{\eta r^3 b}{c} J_1^{oo} \quad (\omega_j - \omega_b)^2 + F_j V_{\xi} \quad \ldots\ldots[4]$$

This form of equation is particularly useful for rapid solutions (eg employing the Mobility concept (18)) as V_{ξ} is directly related to the Mobility Vector M_{ξ} by

$$V_{\xi} = \frac{F(\frac{c}{r})^2 c}{\eta\, bd} M_{\xi}$$

and for short bearing theory (18)

$$M_{\xi} = \frac{(1 - \epsilon\cos\phi)^{5/2}}{\pi} \quad (\frac{d}{b})^2 \quad \ldots\ldots[5]$$

There is a wide range of prediction equations (based on both theory and experiment), for frictional torque, frictional mean effective pressure and power loss, to be found in the literature (2) (8) (16) (19) (20) (21). Many different styles of equation from various sources are shown in Table 3, differing in both format and result.

Table 3 - Power Loss, Friction and Friction Mean Effective Pressure Equations

SOURCE	FORM OF EQUATION	REMARKS
USA BOOKER GOENKA van LEEUWEN (16)	$H = \frac{\eta r^3 b}{c} J_1^{oo} \Delta\underline{\omega}\cdot\Delta\underline{\omega} - \underline{e}\times\underline{F_j}\cdot\underline{\omega} + \underline{F_j}\cdot\dot{\underline{e}}$ $= \frac{\eta r^3 b}{c} J_1^{oo} \lvert\Delta\underline{\omega}\rvert^2 - \lvert e\rvert \lvert F_j\rvert\lvert\bar{\omega}\rvert \sin\phi + \underline{F_j}\cdot\dot{\underline{e}}$	Basis for Table 1 & 2
UK TABLE 1 & 2 (This paper)	$H = \frac{\eta r^3 b}{c} J_1^{oo} (\omega_j - \omega_b)^2 + e F_j \sin\phi \frac{\omega_j + \omega_b}{2} + F_j V \cos\beta$	$\phi_{Martin} = -\phi_{Booker}$ Explains sign change of pressure term
AUSTRIA GROBUSCHEK and EDERER (19)	$N_R(\alpha) = \left[\frac{\eta B D}{\psi}(\omega_w - \omega_s)\frac{\pi}{\sqrt{1-\epsilon^2}} + \frac{\psi\epsilon}{2} P \sin(\delta - \gamma)\right] \times \frac{D}{2}(\omega_w - \omega_s)$ $H = \frac{\eta r^3 b}{c} J_1^{oo} (\omega_j - \omega_b)^2 + e F_j \sin\phi \frac{\omega_j - \omega_b}{2}$	Pressure term differs from Table 1. Believed to be incomplete - see appendix
JAPAN SOMEYA (20)	$N_R^*(\alpha) = N_R(\alpha) + N_R'(\alpha)$ $= \int\int^{B}\int^{2\pi} \left(\frac{h}{2}\frac{\partial p}{\partial\phi} + \eta\frac{U_w - U_s}{h}\frac{D}{2}\right) dz\, d\phi \frac{D}{2}\omega_w$ $+ \int\int^{B}\int^{2\pi} \left(-\frac{h}{2}\frac{\partial p}{\partial\phi} + \eta\frac{U_w - U_s}{h}\frac{D}{2}\right) dz\, d\phi \frac{D}{2}\omega_s - PV\cos\lambda$	Unclear why the term involving ω_s (shell angular velocity) has positive sign
JAPAN NAGAO et al (2)	Friction losses:- crankshaft system $P_{f(c)} \propto \eta L^{0.7} D^3 N C^{-0.5}$	From motored engine
USA BISHOP (8)	$MEP = \frac{B}{S}\frac{N}{1000}\frac{6}{B^3}(a^2 c + b^2 d/m + e^2 f)$	Empirical and from motored engines
UK SPIKES and ROBINSON (21)	$\text{POWER LOSS} = \frac{\eta r^3 \rho\omega^2}{c}\frac{\pi}{\sqrt{1-\epsilon^2}}\left(2 + \frac{3\epsilon^2}{2+\epsilon^2}\right)$	Correlates with experiment (21) (13). ϵ = average eccentricity ratio though

4.5 Method incorporating environmental factors

When studying friction in connecting rod big end bearings three components of load are considered, from reciprocating inertia forces, rotating inertia forces and gas forces due to firing. The reciprocating mass at the small end (consisting of piston, piston pin and part of the connecting rod) together with the rotating mass (remainder of the connecting rod mass) produce the inertia forces acting on the big end bearing. The remaining component is the firing load. Whilst the magnitude of the firing load does not affect the friction very much (a factor of two on firing load may change the friction by only 10 to 20%), it is important that the firing load be considered. The reason for this is that the friction is influenced by the characteristic shape of the journal centre orbit, which is certainly very much modified if one neglects the firing load completely. Martin, Booker and Lo (22) studied the influence of engine inertia forces on power loss in connecting rod bearings and found that the inertia components of load alone were not sufficiently descriptive for power loss prediction.

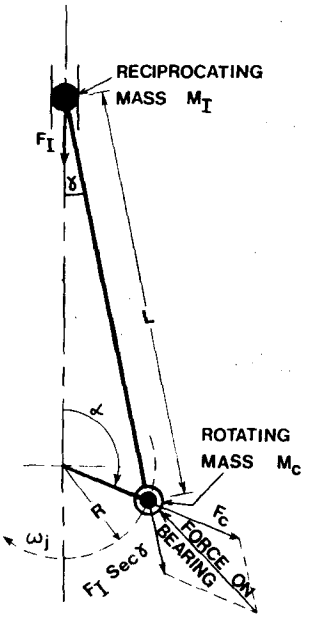

Fig 7 Reciprocating and rotating mass system

Power loss prediction charts are presented in a very general form for a range of bearing length to diameter ratios (b/d from 0.4 to 0.6) in Figs 8 and 9. These charts can be used outside this range (for b/d from 0.2 to 0.7) with little loss in accuracy. The characteristic shapes * of most big end bearing load diagrams have been allowed for by defining them in terms of an inertia shape factor B/A and a firing load factor C/B.

*Footnote - In this study the polar load diagrams are relative to the connecting rod axis and have an 'elliptical' inertia loop; a pear shaped inertia loop is obtained when the load diagram is plotted relative to the cylinder axis (6).

The values A, B and C are dependent on the reciprocating mass at the small end of the connecting rod M_I (ie the mass of the piston assembly (Fig 7) and part of the rod), the rotating component of mass M_c at the big end and the maximum cylinder pressure P_{cyl}.

The load diagram shape ratios can be calculated from:-

$$B/A = (M_I/M_c) + 1$$

and $$C/B = (C/A) \times (A/B)$$

$$= P_{cyl} A_{cyl}/(2M_c\omega_j^2 R ((M_I/M_c) + 1))$$

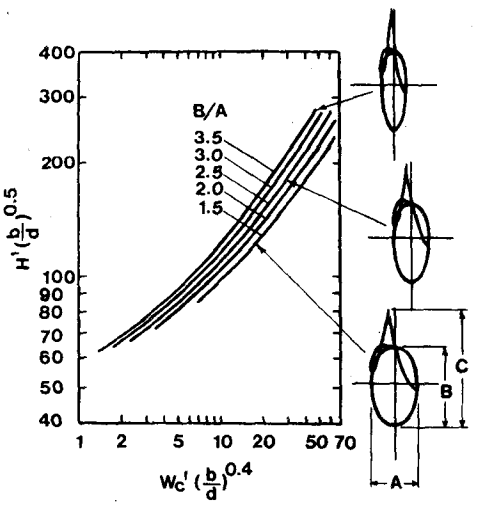

Fig 8 Prediction of power loss in connecting rod big-end bearings; b/d from 0.4 to 0.6; B/A variable; C/B equal to 1.5 (see Fig. 9 for other values of C/B)

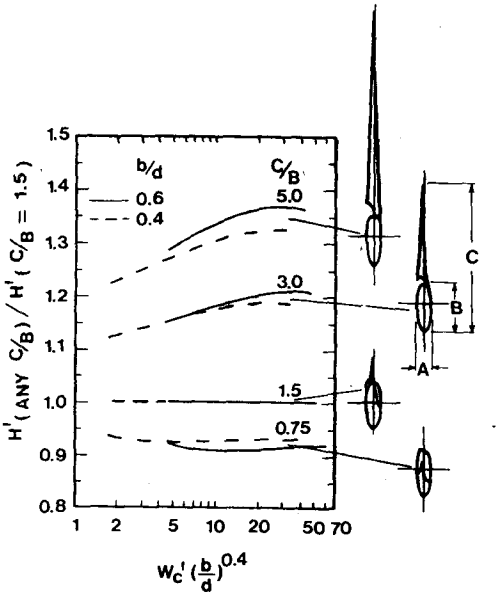

Fig 9 Power loss modifying factor for different C/B ratios b/d from 0.4 to 0.6; C/B variable; B/A from 1.5 to 3.5

Two prediction charts, Fig 8 and Fig 9, have been produced to enable power loss to be estimated. The load diagram shape is represented by the various curves and the load diagram size (using the rotating load component F_c) together with the bearing geometry is represented by the dimensionless load number W'_c. The charts are based on a finite bearing solution and several hundred cases have been computed, for different load diagram shapes and b/d ratios, to arrive at these curves. The dimensionless term H' represents average values of the cyclic variations in power loss.

The b/d terms raised to the power of 0.5 and 0.4 bring all the separate studies for various b/d ratios together. In the same way the power loss modifying factor in Fig 9 corrects the results for different firing loads. As well as giving an immediate assessment of power loss, the design charts are also useful in showing the effect of altering engine and bearing variables (such as piston mass, speed, bearing length, clearance, viscosity etc). Detailed trends are further discussed in a later section of this paper.

5. PREDICTED BEARING FRICTION LOSS FOR THE VEB STUDY CASE

The connecting rod bearing for the Ruston and Hornsby 600 HP, 6 cylinder 600 rev/min VEB MK III diesel engine must be one of the most analysed bearings in the world. The Campbell et al review in 1967 (5) which first used this bearing was mainly concerned with experimental and theoretical predictions of oil film thickness. Subsequently oil flow (6), film pressure (6), (23) and temperature (24) have been considered. However, it is only recently that power loss associated with this particular bearing study has appeared in the literature (25).

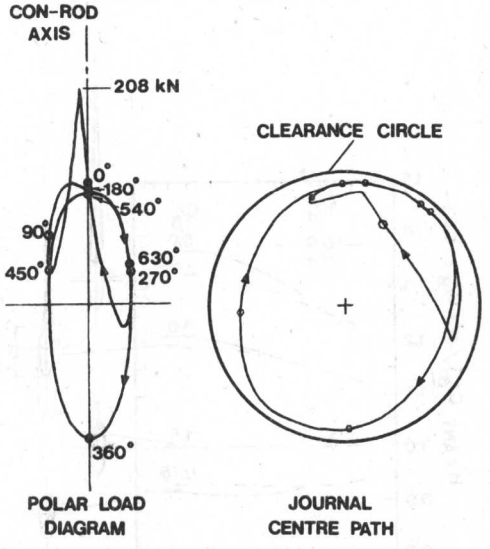

Fig 10 Polar load diagram and journal centre path for VEB connecting rod big-end bearing

5.1 Accumulative factors of friction (hydrodynamic)

The various factors of friction can be specifically defined to match the mathematical terms described in tables 1 and 2. Such terms for the VEB bearing example have recently been computed, for this review, by both the Glacier Metal Company and General Motors Research Laboratories, giving very similar results. A finite bearing mathematical model was used taking into account the oil supply pressure and how it affected the oil film extent (note that this is not the 'film history' case referred to later).

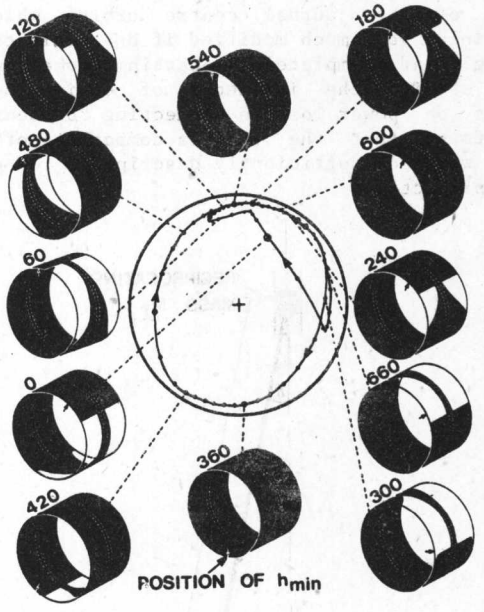

Fig 11 Film extent for VEB study case
Data from General Motors Research Laboratories (26)

Details of the VEB bearing and relevant engine data are given in the Appendix of ref (5). Fig 10 here shows the polar load diagram and a typical journal centre orbit path consistent with previous published results (5) (6). The outer part of Fig 11 shows 'thumb nail' sketches of the oil film extent at every 60 degrees of crank rotation as predicted by General Motors Research Laboratories (26). The circumferential dotted lines represent a full circumferential oil groove, the black area (either side of this) is the predicted film shape (under pressure) and the small arrows indicate the position of minimum oil film thickness for the various crank angle positions. The film shape and film position vary considerably throughout the 720 degrees of crank rotation. At 360, 540 and 600 degrees the bearing is completely full of oil as can be seen from the distribution of the power loss components shown in Fig 12. In this figure (computed by GM) the significance of the various 'mathematical' terms of tables 1 and 2 can be be assessed.

The numbered areas in Fig 12 showing the bearing power loss distribution are related to the power loss terms in Tables 1 and 2 as follows:-

	Fig 12 code	Table 1 and 2
Pressure effect	1	Term B
Translation effect	2	Term C
Shear effect (film as Fig 11)	3	Term A
Shear effect (2π film)	3 + 4	Term A

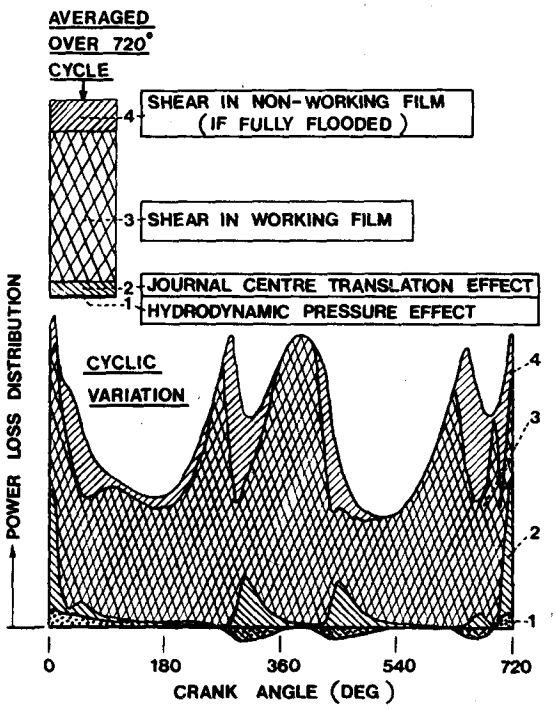

Fig 12 Distribution of bearing power loss for VEB Study case — computed by General Motors Research Laboratories (26)

The hydrodynamic pressure term taken by itself can be negative as well as positive, depending on whether the minimum film thickness position is in advance of or lagging behind the working film. This can be seen in Fig 11 where the minimum film position (small arrow) is in advance at 60° crank angle and lagging at 300° crank angle. This is consistent with the positive and negative values due to the hydrodynamic pressure effect, at these particular crank angles in Fig 12 (shown by the dotted areas). As mentioned earlier the sum of the pressure term and the translation term is independent of the position of the 'observer'. These two terms added together (or the $F_j V_s$ term of equation 4) will always be positive.

The journal centre translation effect is seen, from Fig 12 (area marked 2), to be significant at zero degrees crank angle and this corresponds to the journal centre moving with a high velocity, as shown by the wide spacing of the 10° crank interval markers on the orbit in Fig 11. The shear in the working film is represented by the chequered area in Fig 12 and the total power loss at each individual crank position is given by the summation of the areas marked 1, 2 and 3 (ie the top of the chequered area from the datum) in Fig 12. If instead of having the film extents of Fig 11 the bearing clearance was fully flooded, then an additional component 4 would have to be added to the total. The top line therefore represents the shear effect for a bearing with a 2π circumferential film extent together with the pressure and translation effects. The average values over the full 720° cycle for each of the individual 'components' are shown at the top of Fig 12.

5.2 Comparison of power loss from various sources

Power loss predictions from various sources, for the VEB study case, are compared in Fig 13 and Fig 14a & b. Fig 13 shows the effect of oil film extents using results from various finite bearing solutions. Case (a) neglects the feed pressure and the working film extent is usually just slightly greater than 180 degrees. (Moes and Bosma (27) give a graphical guide for the film extent in dynamically loaded bearings and Goenka has presented curve fit equations (23)). Case (c) is for the theoretical case of a complete film over an angular extent of 2π, including pressure and translatory effects as well as shear. Various computed solutions including the General Motors finite element method (25), Glacier finite difference method (6), and Glacier using Moes

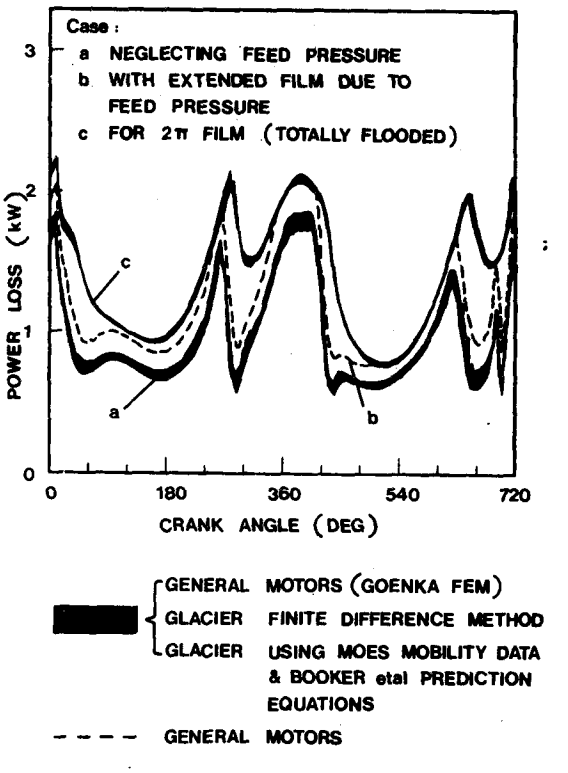

Fig 13 The effects of various film extents on power loss (VEB)

finite bearing mobility data (18) with Booker's Mobility method (18) (5), all lie within the fairly narrow black bands labelled (a) and (c). The intermediate case, curve (b), is from the General Motors results and includes supply pressure effects (film extents as Fig 11).

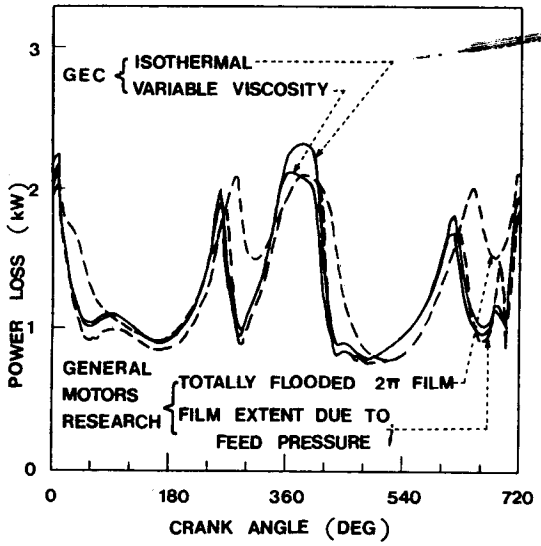

Fig 14a

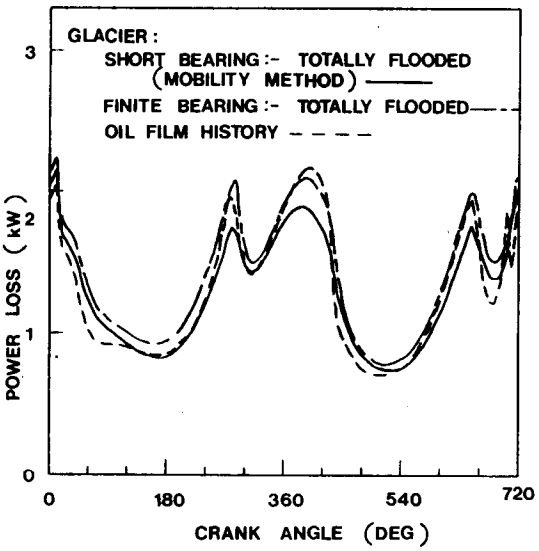

Fig 14b

Fig 14 a & b—Cyclic variation in power loss
—VEB Study case results from different sources

GEC (UK) have also kindly carried out studies for this paper using their optimised short bearing solution (28). This has improved accuracy over the standard short bearing theory especially at high eccentricities and therefore should be more comparable with finite bearing solutions. Unique speed and boundary parameters Ω and α (in place of ϵ, $\dot{\epsilon}$, ω and $\dot{\phi}$ etc) form basic terms in their Reynolds equation. Their equations for power loss can be transformed into a similar form to that shown in tables 1 and 2. GEC's predictions for power loss (29) in Fig 14(a) include the use of a heat balance with variable viscosity (with time); they have also predicted the isothermal case. Furthermore they have attempted (albeit approximately) to take some account of shear in a zero pressure striated film region. Their predictions of power loss for the VEB case are compared with the General Motors result, which are shown by dashed lines in Fig 14a. The GEC cases, with the striated model, would have been expected to be within the General Motors dashed lines, had the eccentricities and viscosities been similar. However with the different models considered the trends are as expected.

Table 4 - PREDICTED POWER LOSS (including hydrodynamic pressure and translation effects) for VEB STUDY CASE

SHEAR FILM EXTENT	TOTAL POWER LOSS kW			
	LOAD CARRYING FILM (NEGLECTING FEED PRESSURE)	CONSIDERING FEED PRESSURE	WITH STRIATED FILM INCLUDED	TOTALLY FLOODED (2π FILM EXTENT)
FINITE BEARING - ISOTHERMAL				
GENERAL MOTORS (FINITE ELEMENT)	1.02	1.19	-	1.39
GLACIER (FINITE DIFFERENCE)	0.97	1.09	-	1.375
GLACIER (MOES MOBILITY MAP)	0.94	-	-	1.39
GEC (OPT. SHORT BEARING)	-	-	1.21	-
GLACIER (OIL FILM HISTORY)	-	0.95	1.29	-
FINITE BEARING - VARIABLE VISCOSITY				
GEC	-	-	1.71	-
SHORT BEARING THEORY				
GLACIER (BOOKER'S MOBILITY MAP)	0.84	-	-	1.26

The cyclic variations of power loss for three different theoretical models are compared in Fig 14b. The 2π film (totally flooded) shear, film pressure and translatory effects are all included in the short and finite bearing models. However, the load carrying film extent is π for the short bearing and slightly greater than π for the finite bearing solution. The finite bearing solution gives higher power losses (chain dashed lines) than the short bearing solution (full line) because of the smaller oil film thickness involved in the former. However the trends are very similar. The third curve (dashed line) is based on a so called 'oil film history' model (15) (6). This involves the study of oil transport within the bearing oil film and

takes into account the effects of insufficient oil to fill the load carrying area of the bearing. Such a theoretical model, which has reduced film extents, has been found to have fairly good correlation with practice, especially for oil flow (6). The reduction in friction that would be gained due to reduced film extent, however, may be offset by increased friction due to resulting smaller oil films. This generally explains why all the curves in Fig 14b have similar trends. Because of the difficulty of defining the shear condition within the striated region, the shear over a complete full width film has been considered; this will predict the upper limit to power loss. The actual shear area may be only slightly less than this for the VEB bearing, since the oil is supplied from a circumferential groove. However, with the more common practice of an ungrooved big end bearing, fed from a crankpin drilling, one would expect less filling of the bearing clearance space. Under such conditions the oil film history model would be more representative of actual performance than the other solutions.

A summary of predicted power loss for the VEB study case is given in table 4, and includes average values for the cases shown in figures 13 and 14a and b from General Motors Research Laboratories, GEC and the Glacier Metal Co.

6. HOW DIFFERENT VARIABLES AFFECT BEARING FRICTION

6.1 Mass of moving parts

The mass of the moving parts in an engine create inertia forces which generally increase friction. However, the reduction of masses is not a simple route to the reduction of friction, as this has to be considered in conjunction with component strength and reliability of performance at the friction producing surfaces. Also vibration and noise may be affected by change in component mass.

The effect of connecting rod mass on the big end bearing power loss can be seen in Figs 8 and 9 for particular cases. The mass system involving the rotating component M_c at the big end and the reciprocating component M_I at the small end is allowed for in the terms B/A, C/B and W'_c. The power loss is mostly affected by the load number W'_c, the b/d ratio and the shape of the inertia loop in the load diagram defined by B/A. Fig 8 involving all of these variables can be used separately (from Fig 9) to obtain a reasonable estimate of power loss. The modifying factor on power loss due to various firing loads, Fig 9, is less significant but nevertheless still important when the value of C/B is high.

The reciprocating mass M_I includes the piston assembly and any weight reduction here could result in lower friction, both at the piston/cylinder interface and at the big end bearing. There will be greater total benefit at the piston, as piston losses form a major part of the mechanical losses. Many designs of lightweight piston have been developed. One novel design developed by Bruni at A E BORGO Spa, Italy (30) is the 'x' piston* shown in Fig 15,

*Footnote – British Patent Application 82.21993 and foreign applications pending.

which has much of the piston skirt removed forming an X shaped support. Such a design will have a small but beneficial effect on the big end bearing friction (due to reduction of B/A ratio in Fig 8).

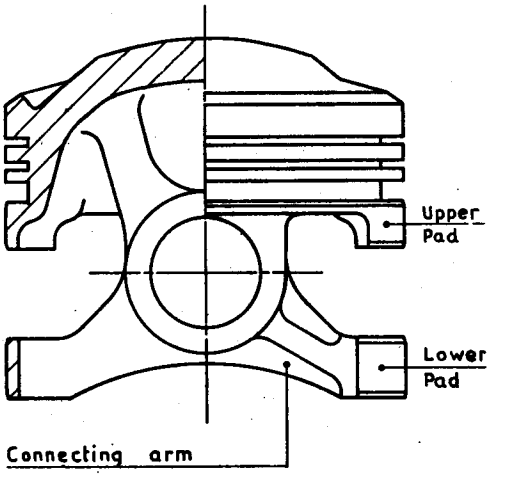

Fig 15 Reduced weight 'x' piston
AE Borgo Spa — Bruni (30)

The effect of reducing reciprocating and/or rotating masses on the connecting rod system will generally result in lower power loss in the connecting rod bearings. Whilst the resultant forces will also change on main bearings these may not necessarily all have a corresponding reduction in friction. In V engines changes in connecting rod mass may require modified balance arrangements which in turn will affect the friction. With all these effects to consider, and engine reliability of prime importance, one cannot be certain of improving the friction in main bearings by changing mass.

6.2 The effect of bearing geometry

The effect of bearing size, operating viscosity and speed on power loss in connecting rod big end bearings can be obtained from Fig 8.

For a quick overall view of trends, however, the author has developed a friction torque trend analyser, Fig 16; this has been derived from the slopes of the B/A curves in Fig 8. In Fig 16 one can see at a glance the likely change in friction torque resulting from a change in any of the variables shown. For instance the example dotted lines show that if the diameter is increased by 50% (a multiplication factor of 1.5), then the resulting frictional torque will be increased by a multiplying factor of between 2 and 2.6. Likewise decreasing the diameter will reduce the friction torque. If two variables are changed simultaneously then the multiplying factor on friction torque will be the product of the two resulting individual factors.

A similar friction torque trend analyser, Fig 17, has been developed for main bearings, by considering measured bearing friction from six